A Low-Noise Current-Mode Preamplifier for Gamma Asymmetry Measurements

W.S. Wilburn [*], J.D. Bowman, and S.I. Penttilä

Los Alamos National Laboratory, Los Alamos, NM 87545, USA

M.T. Gericke

Los Alamos National Laboratory, Los Alamos, NM 87545, USA and Indiana University, Bloomington, IN 47408, USA

Abstract

The NPDGamma experiment will measure with high accuracy a very small parity-violating directional asymmetry A_γ in the emission of gamma rays from the capture of polarized cold neutrons by protons. High event rates and systematic error considerations require the use of current mode detection with vacuum photo-diodes and low-noise solid-state preamplifiers. The preamplifier requirements, design, and measured properties are described.

1   Introduction

The NPDGamma experiment that is under commissioning at the Los Alamos Neutron Science Center (LANSCE) plans to measure the parity-violating di-

[*] Corresponding author. Tel.: +1-505-667-2107. E-mail Address: wilburn@lanl.gov.

rectional asymmetry A_γ in the emission of gamma rays from the capture of polarized cold neutrons by protons [1,2]. The polarization of the pulsed neutrons is reversed periodically by turning on and off a radio frequency magnetic field in a spin flipper. The polarized cold neutron beam is incident on a liquid para-hydrogen target where most of the neutrons are captured by protons. The 2.2 MeV gammas from the capture reaction are detected by an array of 48 CsI scintillators, measuring approximately $15 \times 15 \times 15$ cm^3 [3]. A_γ is expected to be very small, approximately 5×10^{-8}, requiring both collection of a large number of gammas and suppression of systematic effects to below 10% of the expected asymmetry. Meeting these conditions requires that the detector be operated in current mode, its electronic noise be small, and the dynamic range of the signal processing electronics be large. We have designed and built a detector system that meets all these requirements. In this paper we describe a low-noise current-to-voltage preamplifier that is the heart of the detector and discuss its performance.

A current-mode detector system is a prerequisite for successful operation at very high rates. Radiation (2.2 MeV gamma quanta) interacts with a detection medium (CsI) and produces light pulses having a long decay time with components up to 2 μs. The peak rate in each of the 48 detectors is of order 100 MHz and thus the pulses from different events overlap. The overlapping nature of the pulses requires current-mode rather than pulse-mode signal processing. The light signals are converted to current signals by a photo-cathode. The currents are then amplified. The amplification is most often accomplished using a photo-multiplier tube, which has the advantages of providing a large, low-noise gain of up to 10^7.

For the NPDGamma experiment the use of photo-multipliers is precluded by

2

their high sensitivity to magnetic fields. The trajectories of slowly moving electrons that are emitted from the photo-cathode can be deflected by fields of order 1 G to such an extent that they fail to strike the first dynode, causing the gain of the photo-multiplier to be a strong function of the applied magnetic field; a 1 G applied field can change the gain of a photo-multiplier by 100%. In the NPDGamma experiment, a 30 kHz radio-frequency magnetic field having a strength of a few Gauss is used to rotate the neutron spin by 180 degrees. The purpose of the spin reversal is to effectively interchange the role of top and bottom detectors, so that the detector efficiencies do not have to be precisely matched. The physics asymmetry changes sign with neutron spin reversal while the differences in efficiency between detectors do not. In addition, since the spin is reversed at a rate of 20 Hz by turning the RF magnetic field on and off, the effects of detector efficiency drifts with time are suppressed.

In order to reduce the field from the RF spin flipper at the position of the detectors, the spin flipper is enclosed in an aluminum cavity to contain the RF magnetic field. The spin flipper, however, can affect the detectors in two ways. First, the field can induce a signal directly into the detector or associated electronics through magnetic pickup. We refer to this as an additive effect, since it is observed whether or not a signal is present. Second, the field can change the gain of the detector. We refer to this as a multiplicative effect, since it is only observed when a signal is present. These effects are potentially the most dangerous systematic effects because they are correlated with the neutron spin direction. A 1 μG field could change the gain of a photo-multiplier by 10^{-6}, 200 times larger than the goal statistical error of the experiment. For this reason, the scintillation light from the CsI detectors is converted to current by vacuum photo-diodes, and the photo-currents are converted to voltages and

3

amplified by solid-state electronics. The photo-diodes used for NPDGamma have a gain sensitivity to changes in magnetic field of less than 1×10^{-4} G^{-1}, and a second-order sensitivity of less than 1×10^{-5} G^{-2} [4].

Because the gain of the vacuum photo-diode is unity, a preamplifier is needed. Low noise signal processing is required for two reasons. First, we require that the electronic noise (dominated by the preamplifier) be small compared to shot noise arising from the detection of gamma quanta. A second, and more stringent requirement, is that imposed by the need to demonstrate by *in situ* measurement that any false asymmetry of instrumental origin is significantly smaller than the statistical error goal, 10% of the expected physics asymmetry of 5×10^{-8}, on a time scale that is small compared to the experiment running time, a few times 10^7 s. We consider both additive electronic pickup of the reversal signal and possible gain shifts from magnetic fields. The preamplifier that we have designed, built, and tested meets all of these requirements.

2   Concept

The function of the NPDGamma preamplifier is to convert the current from the anode of the vacuum photo-diode to a voltage. The electronic noise of the preamp should be small enough to meet the requirements imposed by the need to demonstrate that instrumental asymmetries are small. The bandwidth should be large enough to give a rise time small compared to a 400 μs averaging interval. The heart of the circuit is an op amp-based current-to-voltage amplifier, shown schematically in Figure 1. Ideally, the transfer function is

simply

$$V_o = -R_f I_i. \tag{1}$$

Noise, however, is inherent to any electrical circuit. If this noise is sufficiently small, the time required to make the measurement is governed by the time needed to collect counting statistics. Otherwise, the measurement time is dominated by the time needed to average the electronic noise. Since NPDGamma is a current-mode experiment, counting statistics is manifest as a shot noise density in the photo-diode current given by [5]

$$i_s = \sqrt{2QI_0}, \tag{2}$$

where Q is the amount of charge created by the photo-cathode per detected gamma and I_0 is the average photo-current per detector. We have measured that gammas interacting in one of the CsI detectors produces, on average, 1.3×10^3 photo-electrons per MeV of deposited energy at the anode [6]. For the 2.2 MeV gammas from the $n+p \rightarrow d+\gamma$ reaction, this gives $Q = 2600e$ and $I_0 = 10$ nA for the expected time-averaged beam intensity of the NPDGamma experiment, giving an average shot noise density $i_s \approx 2$ pA/$\sqrt{\text{Hz}}$.

There are, however, more stringent constraints on the preamplifier noise. It is desirable to take data with the neutron beam turned off to detect the presence of purely electronic systematic effects. Such an effect could arise, for example, from the pickup of the spin-flipper RF power by the detectors, leading to a spin-correlated signal that would mimic a true parity-violating signal. The time required for this measurement is determined by the time required to average the preamplifier noise. We want this time to be much less than the

time required for the beam-on data. The beam-off measurements must be performed in two different modes in order to separately test for additive and multiplicative effects. Additive effects, such as electrical pickup from the spin flipper, directly add to the signal from the physics effect and are best observed when no other signals are present. Multiplicative effects, such as detector gain changes induced by the magnetic field of the spin flipper, require that a signal be present to be observed. We use LEDs mounted on the detectors to produce a DC signal for these tests [6].

The beam-off, LED-off measurement looks for an additive false asymmetry by measuring the pair-wise difference between detector currents integrated over a time T, corresponding to one beam pulse, for a detector in the upper hemisphere of the array Q_{ui} and the opposing detector charge in the lower hemisphere Q_{di}. The difference is then divided by the expected sums of the integrated (beam on) current integrated over a beam pulse $Q_0 = \overline{I}_0 T$ in the two detectors to give the equivalent false asymmetry for one detector pair ε_i

$$\varepsilon_i = \frac{Q_{ui} - Q_{di}}{2Q_0}. \tag{3}$$

The time required to make this measurement to a desired precision can be estimated from the uncertainties in the beam-off measurements, which arise from the preamplifier noise density i_{noise}, $\Delta Q_{ui} = \Delta Q_{di} = \Delta Q = i_{\text{noise}} T \sqrt{f}$, where f is the equivalent bandwidth of the measurement $f = 1/T$, determined by the time during which charge is collected[1]. The uncertainty in the measured

---

[1] The repetition rate of the LANSCE spallation neutron source is 20 Hz. The length of the beam pulse is 50 ms. We do not collect data for the entire 50 ms of each beam pulse. Instead, $T \approx 30$ ms.

asymmetry for one detector pair is then

$$\Delta\varepsilon_i = \frac{1}{\sqrt{2T}} \frac{i_{\text{noise}}}{\bar{I}_0}. \tag{4}$$

Finally, we combine all 24 pairs of detectors to obtain the error in the overall asymmetry for one beam pulse

$$\Delta\varepsilon = \frac{1}{\sqrt{48T}} \frac{i_{\text{noise}}}{\bar{I}_0}. \tag{5}$$

The beam-off, LED-on measurement similarly looks for a multiplicative false asymmetry. In this case, the LEDs are adjusted to produce a DC photo-current comparable to the maximum (peak) photo-current expected during the beam-on measurement. The result is the same as given in equation 5, with one important difference. If the preamplifier noise is sufficiently low (as will be demonstrated in the text that follows), the relevant noise density i_{noise} used in the uncertainty calculation is not that of the preamplifier, but is instead the shot noise density in the photo-current. This shot noise density is given by equation 4 as with the beam-on measurement, except now the quantum Q corresponds to a single electron. For a 10 nA photo-current, the corresponding shot noise density is $i_s = 57 \, \text{fA}/\sqrt{\text{Hz}}$. Applying equation 5, the beam-off, LED-on (multiplicative) false asymmetry is measured to a precision of 4.8×10^{-6} in one beam pulse or 1.1×10^{-6} in one second. The time required to measure the multiplicative false asymmetry to a precision of 5×10^{-9} is 4.5×10^4 s, approximately 12.5 hours.

There are three sources of noise that must be considered in the preamplifier circuit: the Johnson (thermal) noise density e_R in the feedback resistor, and the current i_a and voltage e_a noise densities at the op amp input. Figure 2 shows

7

how these noise sources appear in the circuit, along with parasitic capacitances C_i and C_f. We will consider these noise sources individually. The resistor noise density appears directly at the output and is given by [5]

$$e_R^2 = 4k_B T R_f, \tag{6}$$
$$= R_f \times (1.62 \times 10^{-20} \text{ V}^2/\text{Hz}/\Omega). \tag{7}$$

It can be referred to the input as a current noise density using Equation 1:

$$i_R^2 = e_R^2/R_f^2, \tag{8}$$
$$= (1.62 \times 10^{-20} \text{ V}^2/\text{Hz}/\Omega)/R_f. \tag{9}$$

Applying standard circuit analysis techniques, it can be shown that the voltage noise density of the amplifier appears at the output multiplied by the noise gain of the circuit

$$e_{av}^2 = \frac{C_i}{C_f} e_a^2. \tag{10}$$

Referred to the input,

$$i_{av}^2 = e_{av}^2/R_f^2. \tag{11}$$

Since the three noise sources are independent, their noise densities can be combined in quadrature [5]

$$i_{\text{noise}}^2 = i_R^2 + i_{av}^2 + i_a^2. \tag{12}$$

8

Using values [2] of $R_f = 60$ MΩ, $C_i = 1$ pF, $C_f = 0.05$ pF, $e_a = 2.9$ nV/$\sqrt{\text{Hz}}$, and $i_a = 6.9$ fA/$\sqrt{\text{Hz}}$, we obtain

$$i_R = 16 \text{ fA}/\sqrt{\text{Hz}}, \tag{13}$$
$$i_{av} = 1.0 \text{ fA}/\sqrt{\text{Hz}}, \tag{14}$$
$$i_a = 6.9 \text{ fA}/\sqrt{\text{Hz}}, \tag{15}$$

giving an estimated total equivalent noise density at the input of 17.5 fA/$\sqrt{\text{Hz}}$, dominated by the contribution from R_f.

3 Circuit Description

The actual preamplifier circuit is shown in Figure 3. The circuit consists of a power supply (IC1 and associated components), a 90 V bias supply for the photo-cathode consisting of two 45 V batteries in series, and three stages of amplification (IC2, IC3, and associated components). The power supply consists of a 5 V to ±15 V DC-to-DC converter and three stages of LC filtering on the input and each output. The filters are necessary to keep the converter's 400 kHz switching frequency from coupling to the amplifiers. In spite of these filters, a small but observable signal from the switching noise is electrostatically coupled across the filters to the amplifier section. To prevent this coupling, an aluminum plate 16 mm thick with individual cavities machined for each filter stage and for the amplifier section is placed over the circuit board and grounded.

---

[2] R_f is taken from the circuit design value. C_i is an estimate. C_f is chosen to reproduce the observed pulse response in SPICE models. e_a and i_a are taken from the AD745 data sheet.

The first stage of the amplifier is a current-to-voltage amplifier, as described earlier. It is built around an Analog Devices AD745 low-noise op amp with a feedback resistor R_f of 60 MΩ. A trimmer capacitor C_f can be used to limit the bandwidth of this stage. At present, C_f is not used. The next stage, which uses one of the two op amps in IC3 (Analog Devices OP275), is an inverter with a voltage gain of -2.15. The gain of this stage can be changed by selecting a different value of R_g to compensate for variations in photo-cathode efficiency among vacuum photo-diodes. The final stage is a voltage follower which uses the second op amp of IC3. The purpose of this stage is to provide a low-impedance cable driver for the output of the preamp. Between amplifier stages two and three is a single-pole RC filter consisting of R_l and C_l with a time constant of approximately 1 μs. The purpose of this filter is to roll off the voltage noise of the current-to-voltage amplifier so that the next stage of electronics is not saturated by high-frequency noise components.

The power supply is designed to provide ground isolation between the input power and the amplifier section. The ground reference for the preamplifier comes only from the shield of the output cable, avoiding the ground loop that would occur if the ground from the power input were also connected to the amplifier ground on the preamplifier board. In a test run [4], we observed unacceptably large false asymmetries of 1.1×10^{-7} when ground loops were not treated carefully. This isolation is achieved by a DC-DC converter (Texas Instruments DCP010515), which operates in the standard way, generating ± 15 V outputs from a single 5 V input. The price paid for this isolation is noise from the converter's 400 kHz oscillator which must be heavily filtered as discussed above.

4 SPICE Model

A spice model of the preamplifier was constructed which includes all three stages: current-to-voltage, voltage gain, and voltage follower, as described in the previous section. Models for the operational amplifiers were obtained from Analog Devices, and component values were taken from the actual circuit. The source impedance of the vacuum photo-diode was modeled by a 1 GΩ resistor in parallel with a 1 pF capacitor. These values are reasonable estimates. A parasitic capacitance in parallel with the feedback resistor R_f was included and its value of 0.05 pF was selected to match the step response of the actual circuit. This value is not unreasonable.

Three types of analyses were performed using this model. The first, an AC analysis, gives the transfer function of the preamplifier circuit (Figure 4). The transfer function in the frequency range of interest (below 10 kHz), is flat and has the correct value. The second, a noise analysis, gives the noise density as a function of frequency (Figure 5). In the passband, the noise density predicted by the model is 18.7 fA/$\sqrt{\text{Hz}}$, in reasonable agreement with our theoretical estimate of 17.5 fA/$\sqrt{\text{Hz}}$. At higher frequencies, a broad peak in the noise density appears. This peak is intrinsic to the AD745 model provided by Analog Devices, however its position and width are affected by external components. In particular, as R_f is increased, the noise density peak is shifted to lower frequencies. The excess noise density in the passband is probably due to the tail of this peak. Finally, a transient analysis was performed with a 100 nA, 100 Hz square wave current applied to the input (Figure 6), to show the step response.

5 Measured Performance

Three parameters of the preamp were evaluated: noise, rise time, and step response (overshoot). Since most of the signal filtering takes place in the next stage of electronics (sum and difference amplifier), a six-pole Bessel filter which approximates the response of the missing electronics is used. The results are shown both with and without the filter and all values are referred to the preamp input.

The preamplifier noise density is shown in Figure 5 as a function of frequency. Several interesting features appear in the frequency spectra, particularly when the filter is not used. At very low frequencies, the $1/f$ noise of the amplifier can just be seen. Then at approximately 40 kHz there is a large broad peak in the noise density. As mentioned previously, this peak is an intrinsic feature of the AD745. While the qualitative features of this peak agree with the SPICE model, the measured value is substantially higher than predicted. This may be due to the simple model of parasitic components (only one capacitor) used in the model. Finally, at 400 kHz the power converter switching frequency is seen. When the filter is used, the spectrum is much cleaner. Both the amplifier noise density peak and the switching peak are removed, and the only noise appearing above approximately 10 kHz comes from the oscilloscope used in the measurement. If we expand the horizontal axis and convert the vertical scale from logarithmic to linear (Figure 7), we see that the noise density in the passband is approximately 20 fA/$\sqrt{\text{Hz}}$, in reasonable agreement with the value from the SPICE model of 18.7 fA/$\sqrt{\text{Hz}}$. The difference is probably due to the enhanced size of the observed noise density peak compared to calculation. Applying Equation 5, the beam-off, LED-off (additive) false asymmetry is

measured to a precision of 1.7×10^{-6} in one beam pulse or 3.7×10^{-7} in one second. The time required to measure the additive false asymmetry to a precision of 5×10^{-9} is 5.6×10^3 s, approximately 1.5 hours.

The preamplifier step response was measured by injecting a 10 nA_{pp} 100 Hz square wave into the input. The results are shown in Figure 6. Without the filter, the 10–90% rise time is 5.7 μs, with substantial overshoot. With the six-pole Bessel filter, the rise time is increased to 100 μs and the overshoot is almost completely eliminated.

6 Conclusion

The NPDGamma preamplifier meets all of the stringent requirements of the experiment. It converts current from the vacuum photo-diode into voltage with a trans-impedance gain of 129 MΩ. The transfer function is flat from DC to beyond 10 kHz, providing sufficient bandwidth to accurately encode the detector signals. The measured preamplifier noise density of 20 fA/$\sqrt{Hz}$ is much less than the shot noise density associated with the detection of gamma quanta (counting statistics) of 2 pA/$\sqrt{Hz}$. The run time to measure the physics asymmetry is determined by counting statistics and is not increased by preamplifier noise. The preamp noise density is also small compared to the shot noise density, 57 fA/$\sqrt{Hz}$, with the beam off and light emitting diodes on, used to search for multiplicative false asymmetries. The preamplifier noise determines the time needed to demonstrate that additive sources of false asymmetries are small using beam-off, LED-off measurements. The time needed for both kinds of false asymmetry measurements is small compared to the run time for the measurement of the physics asymmetry. The step response (after appropriate

filtering) is good, with almost no overshoot. The rise time of 5.7 μs (100 μs after filtering) is small compared to the averaging interval of the experiment, 400 μs.

7 Acknowledgments

References

[1] J. Bowman, G. Greene, G. Hogan, J. Knudson, S. Lamoreaux, G. Morgan, C. Morris, S. Penttilä, D. Smith, T. Smith, W. Wilburn, V. Yuan, A. Bazhenov, E. Kolomenski, A. Pirozhkov, A. Serebrov, C. Blessinger, G. Hansen, H. Nann, D. Rich, W. Snow, T. Chupp, K. Coulter, R. Welsh, J. Zerger, S. Freedman, B. Fujikawa, T. Gentile, G. Jones, F. Wietfeldt, M. Leuschner, V. Pomeroy, A. Masaike, Y. Matsuda, S. Ishimoto, Y. Masuda, K. Morimoto, E. Sharapov, Measurement of the parity-violating gamma asymmetry a_γ in the capture of polarized cold neutrons by para-hydrogen, $\vec{n} + p \rightarrow d + \gamma$, Tech. Rep. LA-UR-99-5432, Los Alamos National Laboratory (1999).

[2] W. Snow, A. Bazhenov, C. Blessinger, J. Bowman, T. Chupp, K. Coulter, S. Freedman, B. Fujikawa, T. Gentile, G. Greene, G. Hansen, G. Hogan, S. Ishimoto, G. Jones, J. Knudson, E. Kolomenski, S. Lamoreaux, M. Leuschner, A. Masaike, Y. Masuda, Y. Matsuda, G. Morgan, K. Morimoto, C. Morris, H. Nann, S. Penttilä, a. V. P. A. Pirozhkov, D. Rich, A. Serebrov, E. Sharapov, D. Smith, T. Smith, R. Welsh, F. Wietfeldt, W. Wilburn, V. Yuan, J. Zerger,

Measurement of the parity violating asymmetry a_γ in $\vec{n} + p \to d + \gamma$, Nucl. Instrum. Methods A440 (2000) 729.

[3] W. Snow, W. Wilburn, J. B. M. Leuschner, S. Penttilä, V. Pomeroy, D. Rich, E. Sharapov, V. Yuan, Progress toward a new measurement of the parity violating asymmetry in $\vec{n} + p \to d + \gamma$, Nucl. Instrum. Methods A515 (2003) 563.

[4] G. Mitchell, C. Blessinger, J. Bowman, T. Chupp, K. Coulter, M. Gericke, G. Jones, M. Leuschner, H. Nann, S. Page, S. Penttilä, T. Smith, W. S. W. Wilburn, A measurement of parity-violating gamma-ray asymmetries in polarized cold neutron capture on ^{35}Cl, ^{113}Cd, and ^{139}La, Nucl. Instrum. Methods A521 (2003) 268.

[5] See, for example, P. Horowitz, W. Hill, The Art of Electronics, 2nd Edition, Cambridge University Press, New York, NY, 1989.

[6] M. Gericke, et al., Submitted to Nucl. Instrum. Methods A.
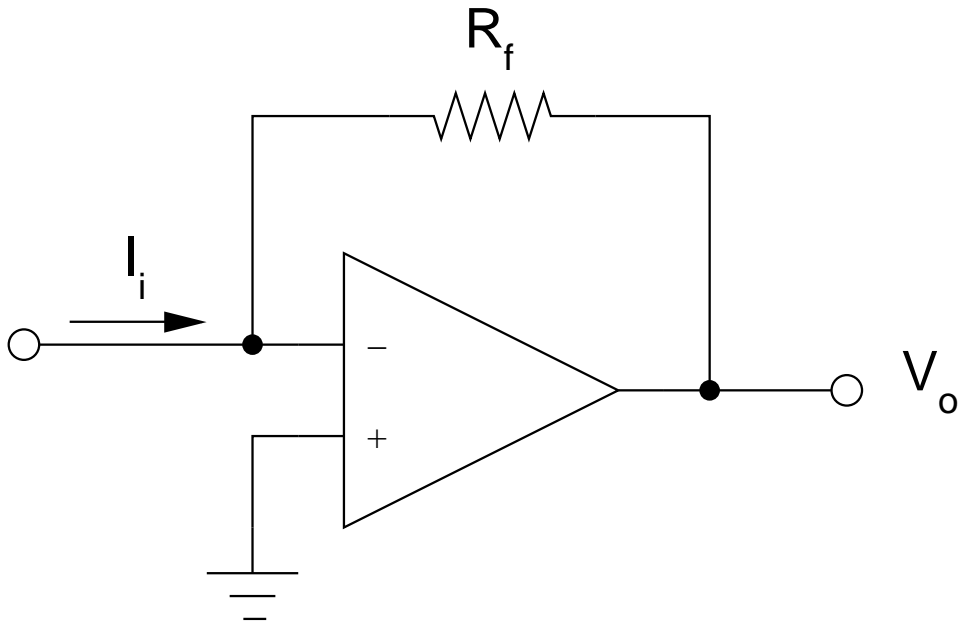
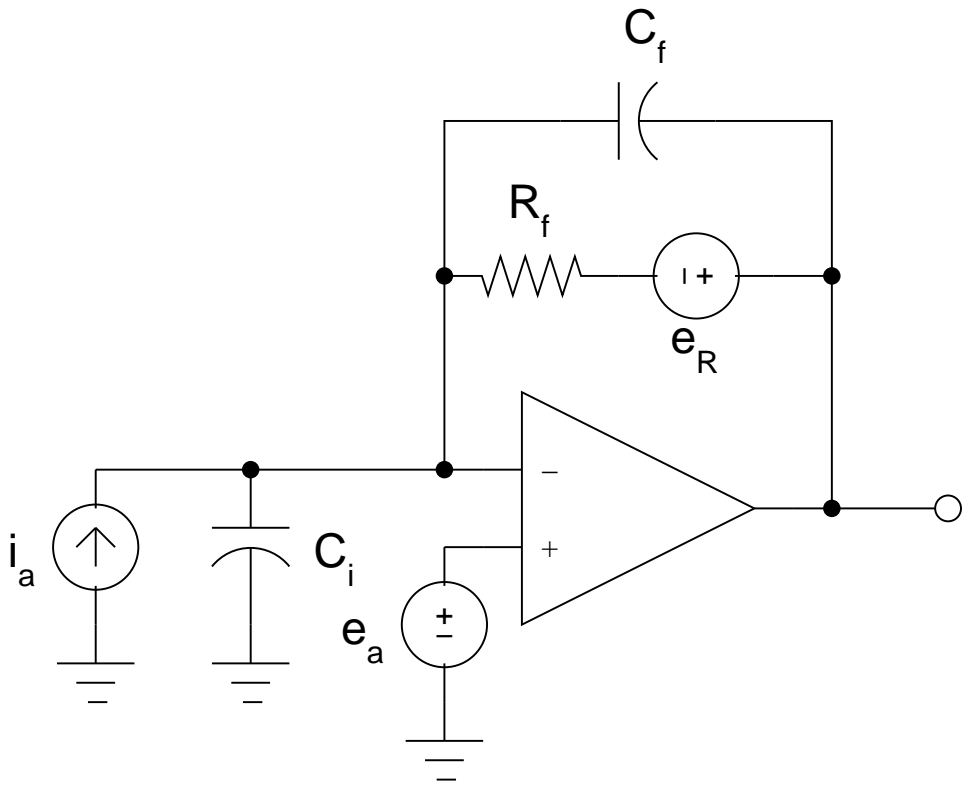Fig. 1. An ideal current-to-voltage amplifier.

Fig. 2. Circuit diagram for a current-to-voltage amplifier including noise sources and parasitic capacitances.
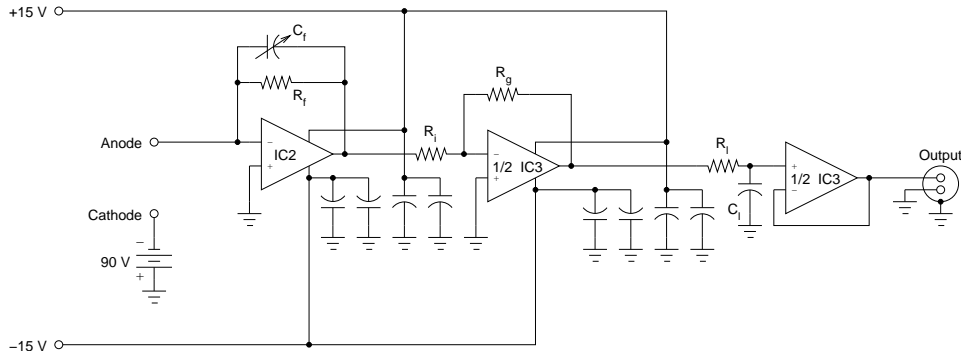
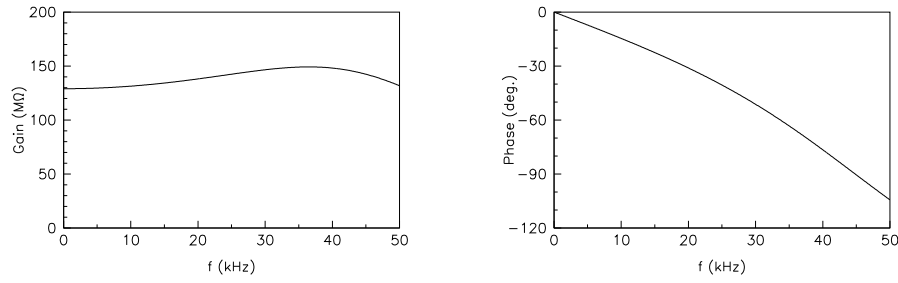Fig. 3. Schematic of the actual NPDGamma preamplifier showing the amplifier stages.

Fig. 4. Transfer function of the preamplifier as predicted by the SPICE model. The left graph shows the magnitude, the right graph the phase.
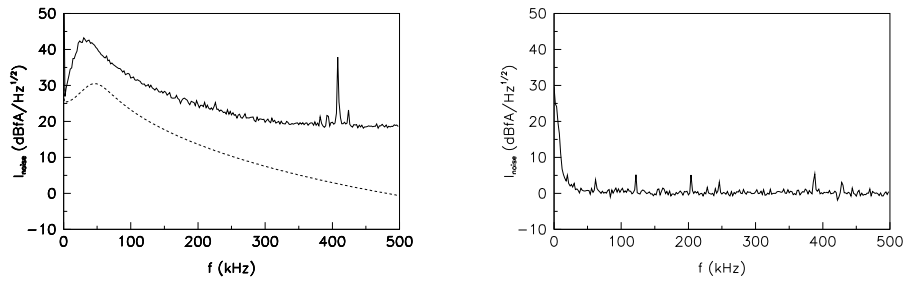

Fig. 5. Preamplifier noise density as a function of frequency without (left) and with (right) filter. The SPICE model prediction (for the case of no filter) is shown as a dashed line.
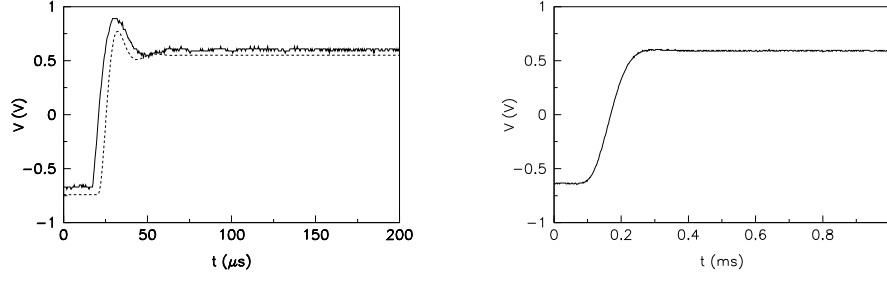
17

Fig. 6. Preamplifier step response without (left) and with (right) filter. The SPICE model prediction (for the case of no filter) is shown as a dashed line.
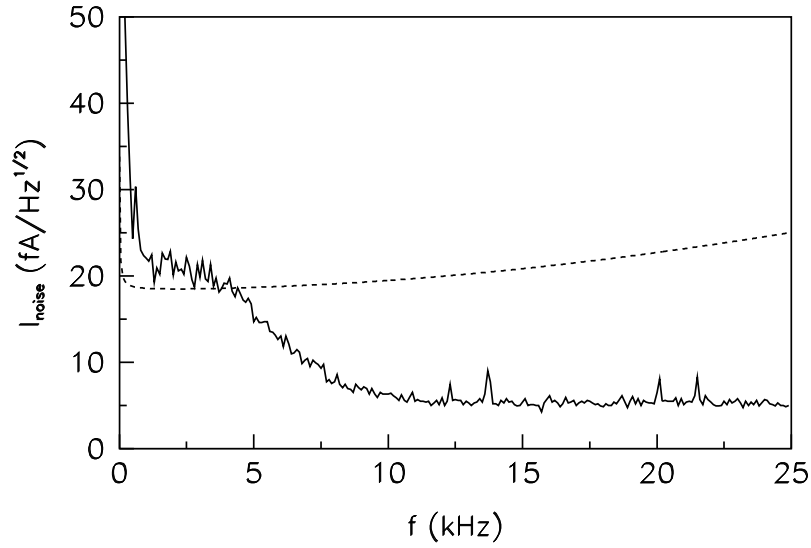

Fig. 7. Preamplifier noise density as a function of frequency (with filter) shown on a linear scale. The SPICE model prediction (which does not include a filter) is shown as a dashed line.